Seeing through the Skin: Photoacoustic Tomography of Skin Vasculature and Beyond

Daiwei Li[1], Lucas Humayun[1], Emelina Vienneau[1,2], Tri Vu[1] and Junjie Yao[1]

Skin diseases are the most common human diseases and manifest in distinct structural and functional changes to skin tissue components such as basal cells, vasculature, and pigmentation. Although biopsy is the standard practice for skin disease diagnosis, it is not sufficient to provide in vivo status of the skin and highly depends on the timing of diagnosis. Noninvasive imaging technologies that can provide structural and functional tissue information in real time would be invaluable for skin disease diagnosis and treatment evaluation. Among the modern medical imaging technologies, photoacoustic (PA) tomography (PAT) shows great promise as an emerging optical imaging modality with high spatial resolution, high imaging speed, deep penetration depth, rich contrast, and inherent sensitivity to functional and molecular information. Over the last decade, PAT has undergone an explosion in technical development and biomedical applications. Particularly, PAT has attracted increasing attention in skin disease diagnosis, providing structural, functional, metabolic, molecular, and histological information. In this concise review, we introduce the principles and imaging capability of various PA skin imaging technologies. We highlight the representative applications in the past decade with a focus on imaging skin vasculature and melanoma. We also envision the critical technical developments necessary to further accelerate the translation of PAT technologies to fundamental skin research and clinical impacts.

JID Innovations (2021);**1:**100039 doi:10.1016/j.xjidi.2021.100039

[1]*Photoacoustic Imaging Lab, Department of Biomedical Engineering, Duke University, Durham, North Carolina, USA; and* [2]*Department of Biomedical Engineering, School of Engineering, Vanderbilt University, Nashville, Tennessee, USA*

Correspondence: Junjie Yao, Photoacoustic Imaging Lab, Department of Biomedical Engineering, Duke University, Durham, North Carolina 27708, USA. E-mail: junjie.yao@duke.edu

Abbreviations: ACD, allergy contact dermatitis; AR-PAM, acoustic-resolution photoacoustic microscopy; CSC, cryogen spray cooling; CSVV, cutaneous small-vessel vasculitis; CTC, circulating tumor cell; FDA, Food and Drug Administration; NIR, near-infrared; OR-PAM, optical-resolution photoacoustic microscopy; PA, photoacoustic; PACT, photoacoustic computed tomography; PAM, photoacoustic microscopy; PAT, photoacoustic tomography; PWS, port-wine stain; RSOM, raster-scan optoacoustic mesoscopy; sO_2, oxygen saturation of hemoglobin; THb, total hemoglobin concentration

Received 22 January 2021; revised 17 May 2021; accepted 28 May 2021; accepted manuscript published online 25 July 2021; corrected proof published online 30 August 2021

Cite this article as: JID Innovations 2021;1:100039

Introduction

Skin is the largest organ in the human body and plays an important role in immunity and regulation (James et al., 2016; Proksch et al., 2008). The skin can be further subdivided into three major layers—the epidermis, the dermis, and the subcutaneous tissue (also known as the adipose layer)—each with its own unique structure and function. The epidermis serves to attenuate harmful UV light from the sunlight using melanin, a natural pigment capable of shielding nuclear DNA from ionizing UVR. The dermis contains hair roots, nerve endings, blood vessels, and sweat glands that regulate body temperature and remove waste products. The subcutaneous tissue provides body energy, reduces external impact, and protects deep tissue. Skin diseases are ranked as the fourth most common cause of global human health issues (Seth et al., 2017). Both neoplastic and inflammatory cutaneous diseases, such as skin cancer, diabetes, and vasculitis, manifest structural and functional changes in the skin, especially in the skin vasculature (James et al., 2016). Currently, a skin biopsy is the standard practice for many skin disease diagnoses; however, this is far from sufficient in clinical practice. First, a skin biopsy cannot evaluate in vivo vascular functions. Increasing evidence has shown that skin diseases often lead to substantial functional changes in the affected blood vessels, resulting in abnormal delivery of oxygenated blood to tissues (Jennette and Falk, 1997; Leder et al., 2013; Maconi et al., 1996; Matteson, 1998; Morris and Beale, 1999; Raza et al., 2000; Schmidt, 2013; Steingräber et al., 2013). Moreover, cutaneous pathology patterns have shown to be highly sensitive to the timing of the biopsy and the age of the lesion. In fact, histology late in the course of skin disease is difficult to interpret by dermatologists because active inflammation often cannot be distinguished from late disease progress. Because of the varied pathogenic mechanisms and the specific organs involved in different skin diseases, a skin biopsy cannot stand by itself; it must be correlated with clinical history, physical and laboratory findings, and skin morphology and function. Therefore, a noninvasive imaging device that can scan skin tissue in vivo would be preferred for skin disease diagnosis. Thus far, clinical skin imaging has been performed with traditional optical imaging methods, including dermoscopy, laser Doppler, optical coherence tomography, and confocal and two-photon microscopy (Arrasmith et al., 2010; Calzavara-Pinton et al., 2008; Funasaka et al., 2013; Ghita et al., 2016; Li et al., 2005). However, the thickness of the skin varies throughout the body, ranging from ~0.5 mm to 4 mm (James et al., 2016), and these optical imaging technologies do not have sufficient penetration depths (Figure 1a). Although ultrasound imaging, another traditional imaging method, can achieve deep penetration, it lacks the sensitivity

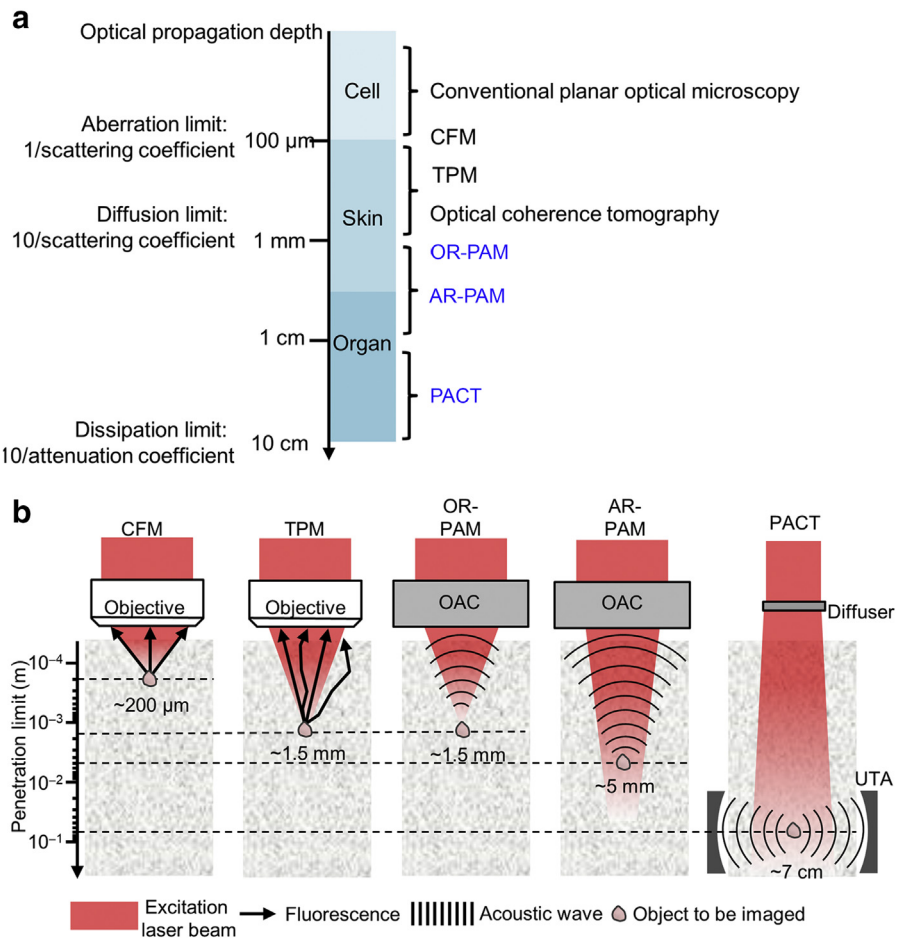

Figure 1. Photon propagation regimes in soft tissue and the penetration limits of representative high-resolution optical imaging modalities. (**a**) Photon propagation regimes in soft tissue and association with the penetration limits of high-resolution optical imaging modalities (Yao et al., 2016). The four regimes are divided at photon propagation depths of approximately 0.1 mm (aberration limit), 1 mm (diffusion limit), 10 cm (dissipation limit), and 1 m (absorption limit), with an optical absorption coefficient of 0.1 cm^{-1}, optical scattering coefficient of 100 cm^{-1}, and anisotropy of 0.9. The classification holds in optical scattering dominant media. Note that the penetration limits shown in this image are order-of-magnitude approximations. (**b**) Signal generation and detection in CFM, TPM, and PAT, with different penetration limits in scattering tissue. Note that the penetration limits shown in the figure are drawn on a logarithmic scale. The colors of the excitation light do not represent the true optical wavelengths. Reprinted with permission from Wang and Yao (2016). AR-PAM, acoustic-resolution photoacoustic microscopy; CFM, confocal microscopy; OAC, optical–acoustic combiner; OR-PAM, optical-resolution photoacoustic microscopy; PACT, photoacoustic computed tomography; PAT, photoacoustic tomography; TPM, two-photon microscopy; UTA, ultrasound transducer array.

to visualize microvasculature without microbubbles. Thus, there is a clinical need for an imaging technology that can provide detailed deep tissue information for skin disease diagnosis and treatment monitoring.

The aforementioned clinical need for skin imaging can be potentially addressed by photoacoustic (PA) tomography (PAT) (Wang et al., 2016). In PAT, excitation light is absorbed by tissue and is converted into pressure waves to form an image. PAT capitalizes on low acoustic scattering of tissue to achieve high spatial resolution at the depths of up to several centimeters (Figure 1b) (Jeon et al., 2016; Yao and Wang, 2013; Zhang et al., 2006b) and has found broad applications in vascular biology (Bitton et al., 2009; Oladipupo et al., 2011a, 2011b), oncology (Chen et al., 2010; de la Zerda et al., 2010; Li et al., 2009, 2008a, 2008b; Olafsson et al., 2010; Staley et al., 2010), neurology (Hu et al., 2009a; Liao et al., 2010; Tsytsarev et al., 2011; Wang et al., 2004), ophthalmology (Jiao et al., 2010; Silverman et al., 2010; Song et al., 2012; Subach et al., 2010; Xie et al., 2009), gastroenterology (Rowland et al., 2012; Yang et al., 2012a, 2012b; Yao et al., 2012a, 2012b), and cardiology (Taruttis et al., 2010; Wang et al., 2010; Zemp et al., 2008; Zhang et al., 2010). Different from traditional optical imaging, PAT uses acoustic detection and thus can penetrate several millimeters into the skin with optically or ultrasonically determined resolutions (Zhang et al., 2006b). By providing high-resolution images with unique optical contrast, PAT has been applied to many preclinical and clinical skin studies. Owing to the unprecedented sensitivity of PA imaging to hemoglobin and melanin, PAT has been commonly used for imaging the vascular system and melanoma. Melanin is abundant in most melanoma cells and provides high contrast images that show the location, shape, and depth of the tumor. PA vascular studies reveal vascular structure, oxygenation, and flow. In the state of disease, these parameters can provide information about the tumor microenvironment, such as angiogenesis and hypoxia. The unique sensitivity of vasculature also helps to detect nonmelanoma skin cancers. In addition, other skin diseases, such as psoriasis, dermatitis, and port-wine stains (PWSs), can be quantitatively detected and evaluated by PAT.

In this concise review, we discuss the technical advances and (pre)clinical applications of PA skin imaging. We introduce the principle of PAT and describe various PA skin

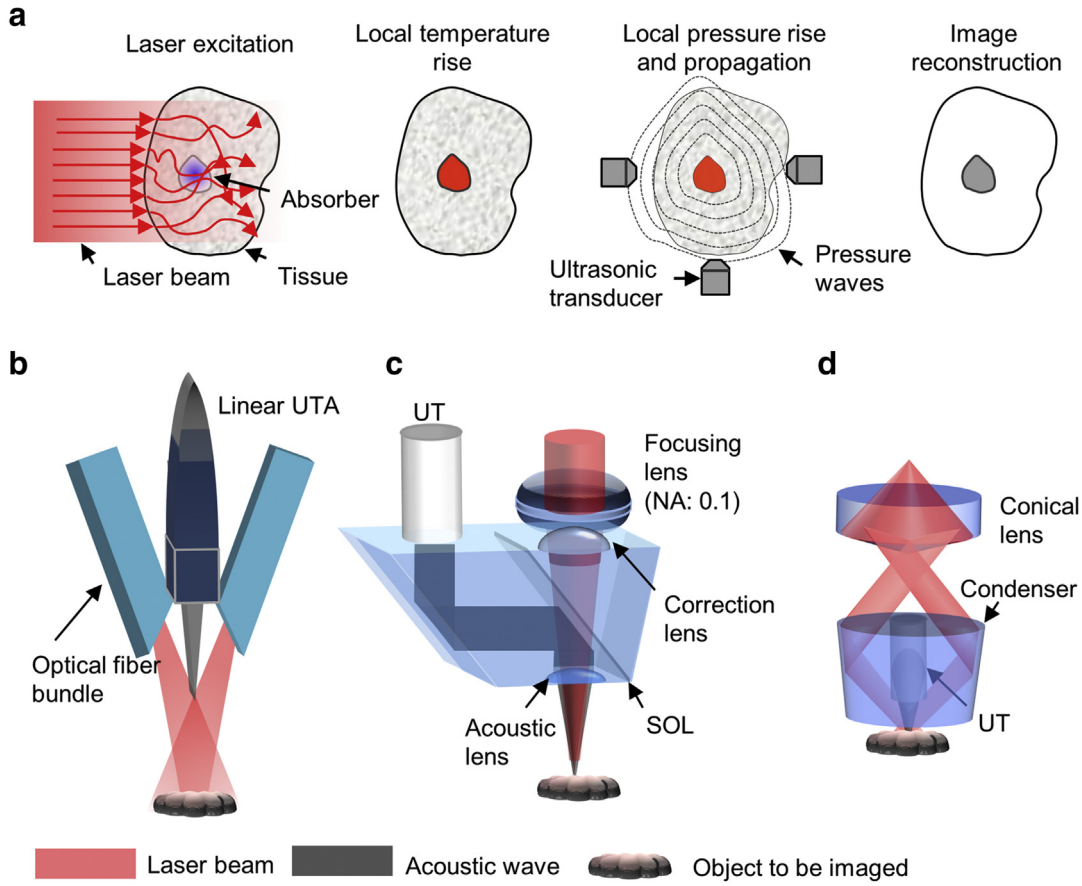

Figure 2. Principles of PAT and major implementations. (**a**) Imaging principle of PAT. When a short laser pulse is fired at the biological tissue, some photons are absorbed by biomolecules, and their energy is converted into heat through the nonradiative relaxation of excited molecules. The local temperature rise induces a local pressure rise, which propagates as an acoustic wave through the tissue and reaches an UT or UTA. The received signals are used to form an image that maps the original optical energy deposition inside the tissue. (**b**) PACT system with a linear UTA (Erpelding et al., 2010), which has been most commonly adapted for clinical studies (Choi et al., 2018). The excitation light is delivered through a fused-end, bifurcated fiber bundle that flanks both sides of the UTA. (**c**) Reflection-mode OR-PAM system with an optical–acoustic combiner that transmits light but reflects sound (Yao et al., 2011). SOL sandwiched between two prisms. OR-PAM is mostly used for preclinical studies. (**d**) AR-PAM system with a dark-field illumination (Zhang et al., 2006b). The laser light is only weakly focused, with the UT in the dark cone. AR-PAM has also been used for the clinical study of skin vasculature disease (Aguirre et al., 2017). Reprinted with permission from Wang and Yao (2016). AR-PAM, acoustic-resolution photoacoustic microscopy; NA, numerical aperture; OR-PAM, optical-resolution photoacoustic microscopy; PACT, photoacoustic computed tomography; PAT, photoacoustic tomography; SOL, silicone oil layer; UT, ultrasound transducer; UTA, ultrasound transducer array.

imaging systems as well as representative PA skin imaging studies. We conclude with a brief discussion of further improvements in PA skin imaging for future clinical translation. In the interest of brevity, only representative technologies and applications are highlighted in this review. Information about more PAT applications can be found in other comprehensive review articles (Attia et al., 2019; Beard, 2011; Cox et al., 2012; Gröhl et al., 2021; Guo et al., 2010; Kim et al., 2010; Manohar and Razansky, 2016; Strohm et al., 2015; Yang et al., 2021; Yao et al., 2010a).

Principles of PAT

Figure 2a illustrates the imaging principle of PAT. To summarize, as photons travel in tissue, some of them are absorbed by molecules, and their energy is partially or completely converted into heat. The heat then induces an initial pressure rise, which propagates as an acoustic wave. An ultrasonic transducer or transducer array detects the acoustic wave to form an image, which maps the original optical energy deposition in the tissue (Wang and Wu, 2007). It should be noted that conventional clinical ultrasound imaging systems often must be modified or optimized for PAT to avoid image reconstruction distortion and to improve the field of view (Choi et al., 2018). PAT has two major implementations on the basis of the image formation methods (Yang et al., 2012c): reconstruction-based PA computed tomography (PACT) and acoustic lens–based PA microscopy (PAM). Both implementations have been used for skin imaging. In PACT, the object is excited by a broadened laser beam. An array of ultrasonic transducers is then placed close to the object to simultaneously receive the emitted ultrasonic waves (Figure 2b). Various reconstruction methods, such as the universal back-projection method (Xu and Wang, 2005) and iteration-based method (Xu and Wang, 2004), can be used to

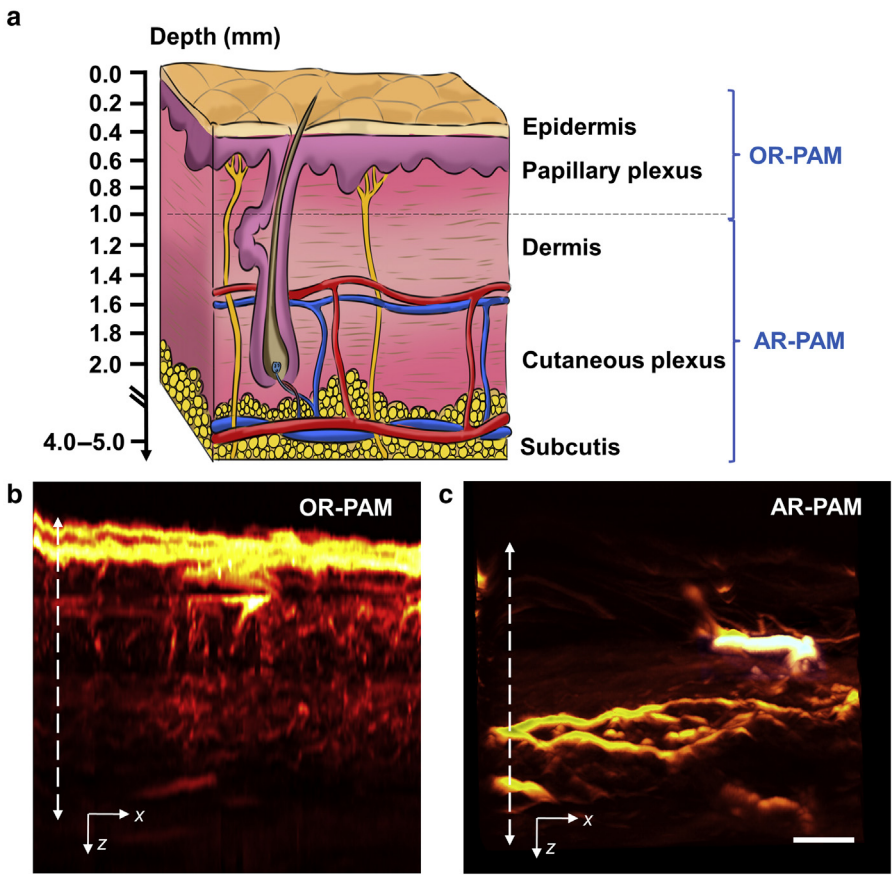

Figure 3. Illustration of the penetration depths of OR-PAM and AR-PAM in the skin. (**a**) Schematic of the skin layers and the corresponding penetration depths of OR-PAM and AR-PAM. (**b**) Representative OR-PAM image of the mouse skin vasculature, showing a 1-mm penetration depth. (**c**) Representative AR-PAM of an ex vivo pig skin sample with blood preserved, showing a 5-mm pentation depth. Bar = 1 mm. AR-PAM, acoustic-resolution photoacoustic microscopy; OR-PAM, optical-resolution photoacoustic microscopy.

map the laser-induced initial pressure rise distribution. Using near-infrared (NIR) light and low-frequency ultrasound detection, PACT can readily achieve a penetration depth of several centimeters, a length that extends deeper than any human skin. In PAM, instead of reconstructing the image digitally as PACT does, a focused ultrasound transducer is used for analog image reconstruction. On the basis of the spatial resolution and targeted imaging depth, PAM generally has two formats: optical-resolution PAM (OR-PAM) (Figure 2c) (Maslov et al., 2008), which has a lateral resolution ranging from submicrometer to a few micrometers and an imaging depth <1.0 mm, and acoustic-resolution PAM (AR-PAM) (Figure 2d) (Maslov et al., 2005), which has a lateral resolution of tens of micrometers and an imaging depth of 1.0–10 mm. The smallest vessels of the skin (known as papillary plexus) are mostly contained within the 1 mm depth of the dermis, and the larger vessels of the subcutis can reach up to 4 mm (Figure 3a); therefore, the papillary plexus can be imaged with single-vessel resolution using OR-PAM (Figure 3b), and the larger vessels of the subcutis can be imaged with deep penetration using AR-PAM (Figure 3c). To capture the highest degree of details and maximize the penetration depths, hybrid systems have been developed to incorporate both OR-PAM and AR-PAM (Ma et al., 2020). Throughout the rest of this paper, we aim to simplify the engineering terminology for clinical readers using PAT in general for different implementations, if not otherwise stated. The readers are encouraged to refer to the corresponding literature for the technical details.

To accommodate the rich optical absorption contrast in biological tissues, PAT has expanded its arsenal of optical excitation wavelengths to provide the most optimized imaging performance, such as detection sensitivity and contrast to noise ratio (Upputuri and Pramanik, 2020; Yao and Wang, 2014, 2013). Hemoglobin in red blood cells is the major optical absorber that provides the high image contrast of blood vessels (Hu and Wang, 2010). The visible light wavelength ranging from 500 nm to 650 nm is most often used for PAT of skin vasculature, balancing between the penetration depth and the signal to noise ratio. The distinct features in the optical absorption spectra of oxyhemoglobin and deoxyhemoglobin allow for multispectral unmixing of the two forms. Melanin has a broad and relatively featureless optical absorption spectrum ranging from visible light to NIR light and thus is often imaged by PAT at wavelengths longer than 750 nm to suppress the background signals from hemoglobin (Park et al., 2021; Staley et al., 2010). DNA and RNA in the cell nuclei have strong optical absorption in UV light and can be imaged by PAT at wavelengths around 200–300 nm (Haven et al., 2020; Wong et al., 2017a, 2017b; Yao et al., 2010a). Water and lipids have relatively strong absorption in the far NIR or mid-infrared region and can be imaged by PAT at wavelengths >1,200 nm (Pleitez et al., 2020; Shi et al., 2019).

Biomarkers for functional PAT

Alongside its ability to penetrate deep into the skin to visualize vasculature, PAT is also powerful in its inherent

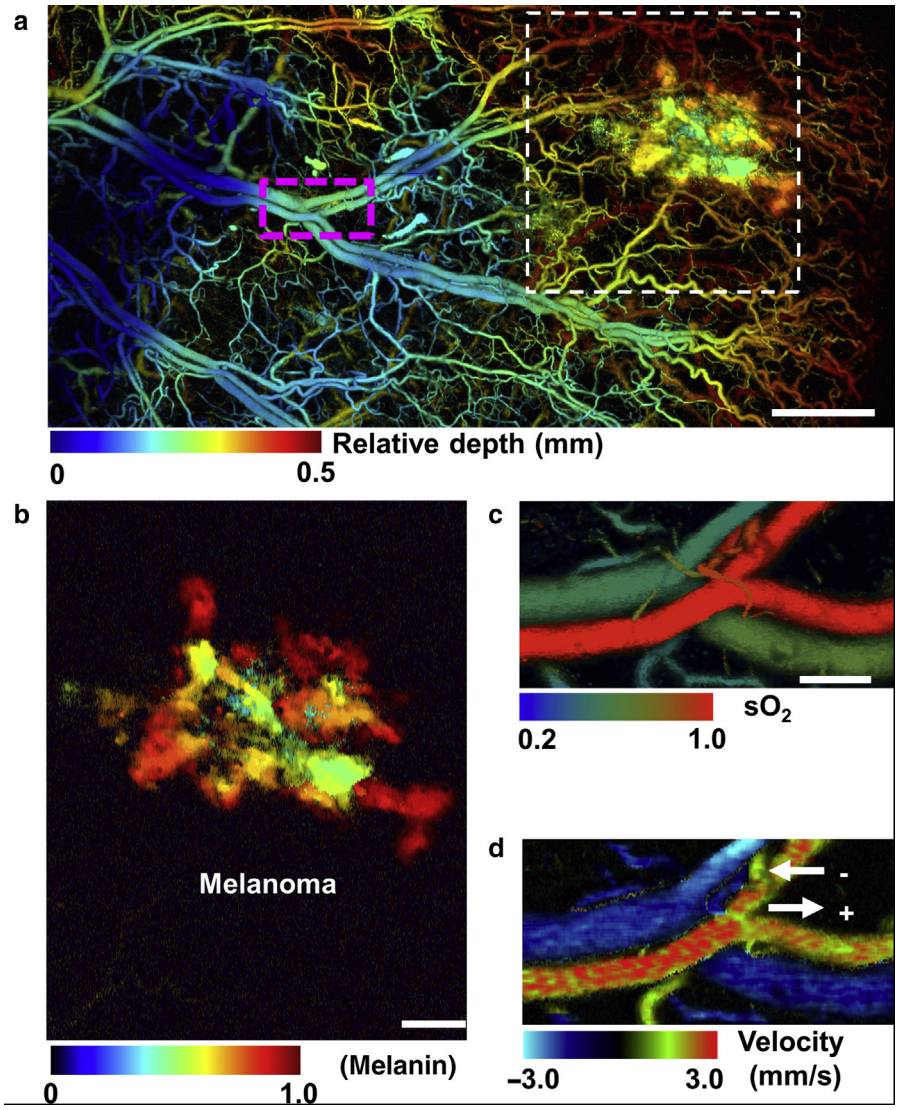

Figure 4. Representative PA imaging of skin vasculature using endogenous contrast. (**a**) PA microvasculature imaging of a mouse ear bearing an implanted B16 melanoma tumor. Depth is coded by colors: blue (superficial) to red (deep). Bar = 1 mm. (**b**) Close-up PA image of the B16 melanoma tumor identified in the white box of **a** using spectroscopic measurements. (**c**) PA sO2 imaging of the principal arterial–vein pair. Bar = 200 μm. (**d**) PA flow velocity imaging of the principal arterial–vein pair. PA, photoacoustic; sO_2, oxygen saturation of hemoglobin.

sensitivity to a variety of functional and molecular biomarkers. In fact, as shown in Figure 4, PAT can be used for functional imaging of blood vessels surrounding a melanoma tumor by quantifying the vascular density, oxygen saturation of hemoglobin (sO_2), and blood flow speed. In this example, the spatial resolution of PAT is sufficient to resolve single capillaries and even red blood cells (Figure 4a). PAT is also capable of quantitative analysis of tissue components with spectroscopic measurement, such as the melanin concentration in the melanoma tumor (Figure 4b). Because PAT exploits the absorption properties of biomolecules to generate contrast, functional information of the hemodynamics can be obtained without injecting any contrast agents. For example, sO_2 is an important biomarker for skin cancer prognosis, treatment monitoring, and wound healing monitoring. PAT can provide high-resolution sO_2 measurements using hemoglobin as the endogenous contrast (Figure 4c). In fact, sO_2 has been successfully imaged by PAT at different length scales in a number of cases, including during cuffed occlusion of the arm (Favazza et al., 2010), controlled temperature changes (Favazza et al., 2010), and relatively homeostatic situations (Deán-Ben and Razansky, 2014; Favazza et al., 2011; Zhang et al., 2007a, 2006a, 2006b). sO_2 has even been resolved down to the single-cell level in a human cuticle (Hsu et al., 2016). The total hemoglobin concentration (THb) can also be calculated at an isosbestic wavelength, where deoxyhemoglobin and oxyhemoglobin have identical molar extinction coefficients (Patrikeev et al., 2007).

Blood flow velocity is another critically important biomarker of vascular function and tissue viability. Although Doppler ultrasound techniques have proven useful for large veins and arteries, these techniques do not work well for smaller blood vessels and low flow speeds. In PAT, the Doppler effect can be utilized to measure flow speed. Yao et al. (2010b) showed that Doppler bandwidth broadening can be measured and can be related to the velocity of transverse blood flow. Once it was determined that flow rate could be measured with PA imaging, researchers sought to measure the metabolic rate of oxygen, another critical biomarker of tissue health. This parameter encompasses vessel geometry and weight, THb, oxygen saturation, and flow rate, all of which can be measured by

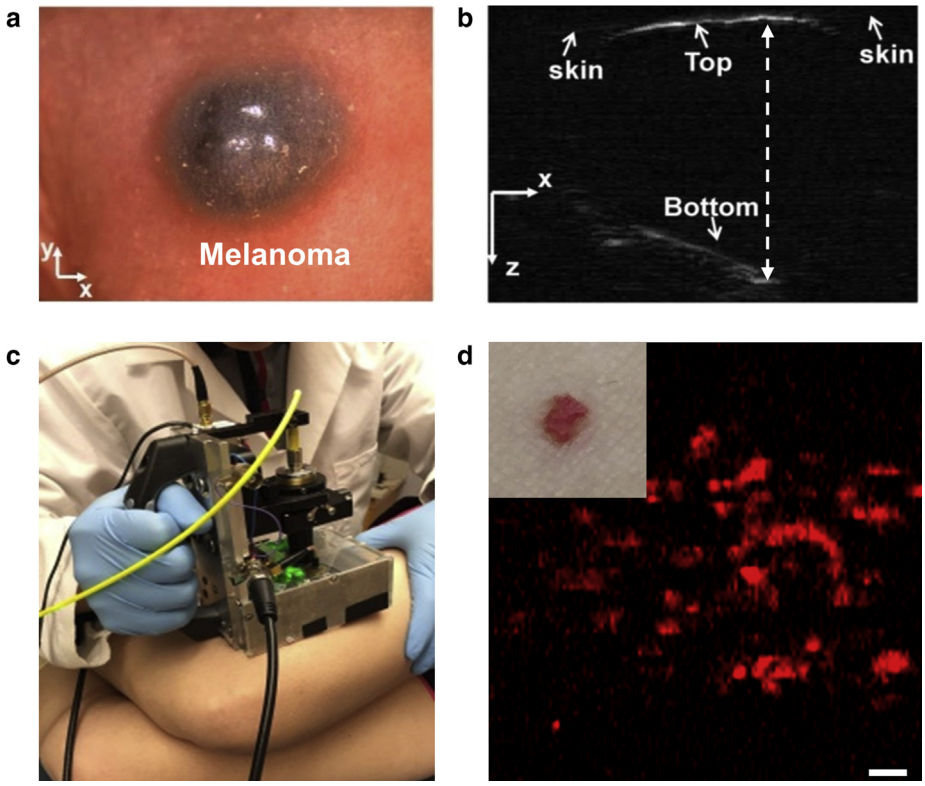

Figure 5. PAT of melanoma and pigmented lesion. (**a**) Photograph of the melanoma in a nude mouse in vivo. Bar = 1 mm. (**b**) Handheld PAM of melanoma clearly shows both the top and bottom boundaries. The dashed line indicates 3.6 mm. Bar = 1 mm. (**c**) Photograph of handheld PAM imaging a red mole on a volunteer's leg. (**d**) A handheld PAM image of the mole reveals an irregular blood vessel pattern. The inset shows the photograph of the mole. Bar = 1 mm. Reprinted with permission from Lin et al. (2017) and Zhou et al. (2015). PAM, photoacoustic microscopy; PAT, photoacoustic tomography.

PAT alone. Because the metabolic rate of oxygen indicates the rate at which tissue is consuming oxygen, it is valuable for cancer diagnosis and treatment evaluation (Yao et al., 2011). At clinically relevant depths, PAT can be potentially an invaluable tool to study skin disease and treatment.

Applications of PAT for skin imaging

Although each skin disease possesses its own unique properties, almost all skin diseases are characterized by neovascularization or changes in vascular function (Miller and Mihm, 2006). Since the first demonstration of PAT of human palm vasculature at an imaging depth of 4 mm (Zhang et al., 2009), PAT of the skin vasculature has become a valuable tool for detecting and characterizing various skin conditions. In fact, many vascular details, including thickness, diameter, and depth, can be obtained through the use of PA dermoscopy (Xu et al., 2016). In this section, we will review the different ways through which PAT has been applied in preclinical and clinical studies of skin diseases on small animal models and patients.

PAT of melanoma. Melanoma is the deadliest form of skin cancer projected to claim the lives of 7,180 Americans diagnosed in 2021 alone, according to the 2021 melanoma skin cancer statistics by the American Cancer Society. Characterized by the dysregulated division of melanocytes due to an accumulation of mutations in genes responsible for cell division, melanoma can be lethal if allowed to metastasize (Davis et al., 2019). Thus, the best way to reduce mortality is through the detection of early-stage melanoma before metastasis. In fact, according to the Melanoma Research Alliance, patients with localized melanoma (stages 0, I, and II) have a 5-year survival rate of 98.4% in comparison with the 5-year survival rate of patients with metastatic melanoma who have a survival rate of only 22.5%. In clinical practice, a biopsy may be performed to identify malignant lesions, but the diagnostic accuracy of a given biopsy depends largely on the skill and experience of the doctor. In fact, the diagnostic certainty of an early stage in situ melanoma is only 73% for excisional biopsy, 75% for deep shave, 44% for punch, and 42% for superficial shave (Hieken et al., 2013). Given the large margin of diagnostic error in biopsies, there is clinical value in looking for diagnostic alternatives.

PAT presents itself as a viable diagnostic alternative to biopsy. PAT is extremely sensitive to melanin's strong light absorption over the NIR wavelength spectrum, and it is capable of penetrating the dermis, making it an ideal method for longitudinal monitoring of melanoma. It is also worth noting that other pigmented lesions can be characterized by PAT, including seborrheic keratosis and dysplastic nevi, both of which are benign and are commonly mistaken for melanoma. In fact, PAT has shown success in delineating the lower boundary of pigmented lesions, revealing the lesions propensity for further invasion (Figure 5a and b) (Breathnach et al., 2015; Schwarz et al., 2015). Zhang et al. (2006a) were among the first to use dual-wavelength PAT to perform functional imaging on mouse models of melanoma (Oh et al., 2006; Zhang et al., 2006b). Zhou et al. (2015) showed the volumetric melanoma growth rate over the course of tumor progression in nude mice in vivo, which was extremely useful for diagnosis, staging, and treatment evaluation.

In addition to elevated melanocyte activity, melanoma is also characterized by neovascularization, with linear irregular vessels as the most common vascular structure (33.3%), followed by punctate vessels and polymorphic/atypical vessels (Argenziano et al., 2004). In fact, Omar et al. (2015) used AR-PAM to study the vascular network supporting the growth of melanoma through several millimeters of tumor depth. The principles of PA imaging of melanoma vasculature can also be extended to other skin carcinomas. For example, Zhou et al. (2017) successfully conducted all-optical integrated PA optical coherence tomography to gather in vivo imaging of basal cell carcinoma and analyze its vascular morphology.

Success in preclinical melanoma research by PAT has since seen applications in the clinic. Chuah et al. (2017) showed a high histological agreement of melanoma depth measurements with multispectral PAT in three human patients. Kim et al. (2018) later showed the utility of PAT in assessing the margins of human tumor resections ex vivo. Dual-wavelength imaging has also been performed on humans using the commercial PAT system Vevo Lazr (Breathnach et al., 2015). Park et al. (2021) showed success in identifying the depths of in situ and nodular melanoma as well as surrounding neovascularization in six patients in vivo using a three-dimensional multispectral PA imaging system. As of late, melanoma diagnosis has even seen further advancement through the development of handheld PAT systems (Figure 5c and d) (Chuah et al., 2017; Lee et al., 2020; Zhou et al., 2015). In addition, PAT has been applied to melanoma detection in conjunction with other imaging modalities, such as optical coherence tomography (Rahlves et al., 2016) and ultrasonography (Wang et al., 2016). Acknowledging its function and flexibility within the expansive field of diagnostic imaging technologies, it is likely that PA systems will soon find a place in the field of melanoma diagnosis.

PAT of other skin disorders. Psoriasis is a chronic inflammatory skin disease that presents in the majority of affected individuals as irritated patches of red skin covered in white scales or plaques. It is typically characterized by dysfunction of the immune system, which causes sustained inflammation and subsequent dysregulated division of keratinocytes. One of the main concerns with psoriasis is the progression of the disease to psoriatic arthritis, which impacts up to 40% of patients with psoriasis and causes pain and swelling of the joints (Rendon and Schäkel, 2019). Although there is no known cure for psoriasis, several viable treatments include topical steroid creams, phototherapy, retinoids, and immunosuppressant prescription drugs (Kim et al., 2017). Because psoriasis diagnosis is primarily clinical, subtle changes indicating the onset of psoriatic lesions can go unnoticed. In fact, epidermal hyperplasia in patients with psoriasis is preceded by extensive angiogenesis in the superficial dermis (Heidenreich et al., 2009). These changes in vasculature can be distinguished from nondiseased skin. In fact, electron microscopy was used to identify capillary loops that curl around the papillary vessel and are closely enveloped by the epidermis as a strong indicator of early psoriatic angiogenesis (Braverman and Yen, 1977; Ryan, 1980). Because PAT can successfully visualize vascular structures at large depths in tissue, it has shown great potential for application in early psoriasis diagnosis. Whereas low-sensitivity PA systems appear to be outperformed by other imaging alternatives such as confocal microscopy (Ossadnik et al., 2018), advances in ultrasound transducers (Wang et al., 2020) demonstrate that high-sensitivity PA imaging modalities can be used to study psoriasis-derived changes in vasculature. In fact, Aguirre et al. (2017) used a portable raster-scan optoacoustic mesoscopy (RSOM) system to provide quantitative vascular analysis of psoriasis progress, including increased vessel density and capillary bending in the upper dermis, with high sensitivity and high resolution (Figure 6).

Dermatitis describes a class of skin diseases that involve irritation of the skin manifesting in rashes as a result of inflammation. Allergy contact dermatitis (ACD), a subset of dermatitis cases, affects around 15–20% of the general population (Thyssen et al., 2007) and is typically triggered by the innate and adaptive immune responses to the infiltration of the epidermal layer by an exogenous irritant (Martin, 2012). In diagnosing ACD, physicians typically employ patch testing to identify the specific allergens associated with flare-ups. Unfortunately, there is a large margin of error in patch testing because test results are subjectively determined by a physician's visual assessment, and skin irritation may be the result of the patch test itself rather than that of the allergen being tested. In fact, positive tests were only reproducible in 86% of cases, and the reproducibility was far lower for mild reactions (Lazzarini et al., 2013). However, using RSOM, Hindelang et al. (2020) were able to distinguish between mild (+) and strong (++) reactions to patch-tested allergens using vessel fragmentation and the ratio of low- to high-frequency content as biomarkers. Although Hindelang et al. (2020) are one of the first to explore PAT in patch testing, their results are promising for future applications of PAT to diagnose this disease. In fact, preliminary studies of RSOM in atopic dermatitis (eczema) have already shown greater strength than the studies of optical coherence tomography in identifying disease severity (Yew et al., 2021).

PA imaging has also been applied to the study of PWS because it is associated with many malformed venules concentrated in the superficial dermis of the affected area. PWSs are reddish birthmarks that can appear anywhere on the body and are due to excessive vascularization of the capillaries. The most common form of treatment is laser therapy to coagulate the unnecessary capillaries causing the redness. This is often paired with simultaneous cryogen spray cooling (CSC) of the epidermis to protect it from overheating. However, to optimize treatment parameters and guide the laser to the optimal focal points, accurate depth and morphology of PWS vascularization are necessary. In a series of studies, Viator et al. (2009, 2003, 2002a, 2002b) developed a PA imaging system to study the excessive blood vessels and capillary malformation in PWS and to quantify the PWS thickness for laser treatment planning. Using PAT, CSC and laser therapy can be adjusted appropriately to remove as much of the PWS as possible while still preserving the epidermis.

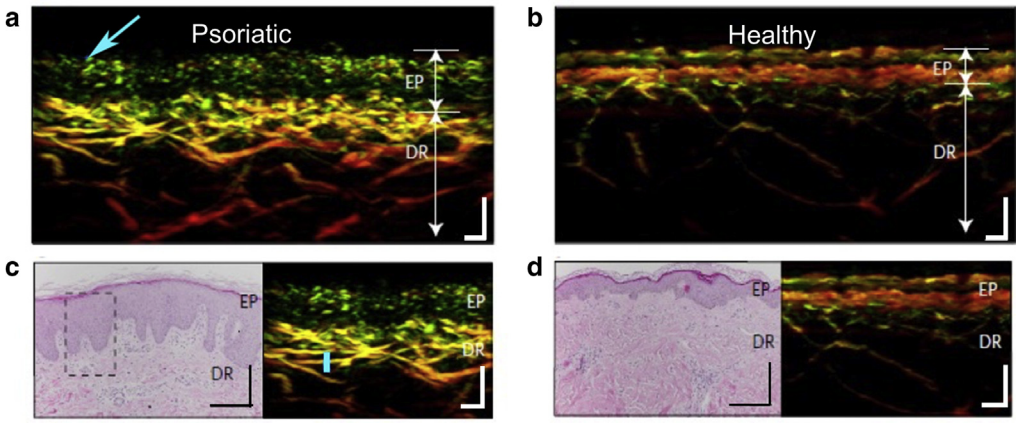

Figure 6. AR-PAM of healthy skin versus that of adjacent psoriatic skin and validation by histology. (**a**) Cross-sectional AR-PAM image of psoriatic skin showing the top part of elongated capillary loops (cyan arrow) that almost climbed to the skin surface through elongated rete ridges. Bar = 200 μm. (**b**) Cross-sectional AR-PAM image of adjacent healthy skin showing a layered EP structure with clearly resolved vessels in the DR. Bar = 200 μm. (**c**) Histology image (left) of the psoriatic skin and the corresponding AR-PAM cross-sectional image (right). The histology image shows the acanthosis, the elongated capillary loops through the rete ridge, and the increased vascularization of the DR. Bar = 300 μm. (**d**) Histology image (left) of healthy skin and the corresponding AR-PAM cross-sectional image (right). Bar = 300 μm. Reprinted with permission from Aguirre et al. (2017). AR-PAM, acoustic-resolution photoacoustic microscopy; DR, dermis; EP, epidermal.

PAT of burn injury and wound healing. Evaluating burn injury and monitoring its healing process are other important medical applications of PAT. Burn injury is commonly induced by excessive heat exposure, and severe burn is life threatening. In the United States only, >400,000 burn injuries need medical treatment annually, leading to >3,000 deaths (Crowe et al., 2019). Surface area and depth of the burn are the two most important indicators for the prognosis of a patient with a burn. Whereas the burn surface area is relatively simple to measure by visual examination, the burn depth is much more challenging to precisely evaluate. An accurate burn depth is a valuable information to decide whether skin grafts are necessary and guide the clearance of necrotic tissue.

Using only hemoglobin and water as the endogenous contrast, PAT has the potential to characterize the pathological features of healthy skin, superficial dermal burns, deep dermal burns, and deep burns (Sato et al., 2005, 2001; Yamazaki et al., 2005, 2003, 2002). There are several recent studies using PAT for burn injuries, which have majorly focused on establishing the technical feasibility, enhancing the system performance, and collecting preliminary data to support future clinical trials. For acute burns, PAT can clearly delineate the hyperemic bowl, the boundary between the edemic coagulated burned tissue and the healthy perfused tissue (Figure 7a and b) (Zhang et al., 2007b, 2006c). Ida et al. (2016) recently compared the PAT measurement of burn depth with laser Doppler measurement and have found that PAT is more accurate, especially in burns induced by high temperature. Talbert et al. (2007) reported that PAT can distinguish coagulated blood from normal blood using spectral measurements. The coagulated blood is often

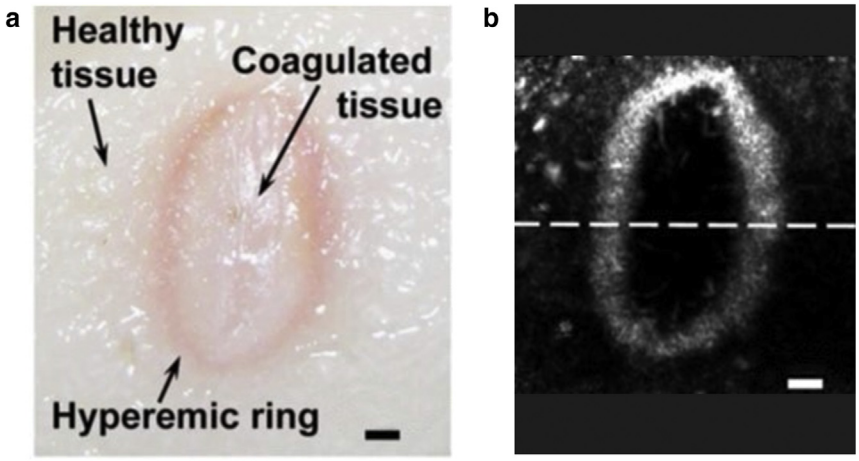

Figure 7. PAT of burn injury. (**a**) Photograph and (**b**) AR-PAM image of an acute skin burn induced by 175 °C heat exposure for 20 seconds, showing the characteristic hyperemic ring. Bar = 1mm. Reprinted with permission from Zhang et al. (2006c). AR-PAM, acoustic-resolution photoacoustic microscopy; PAT, photoacoustic tomography.

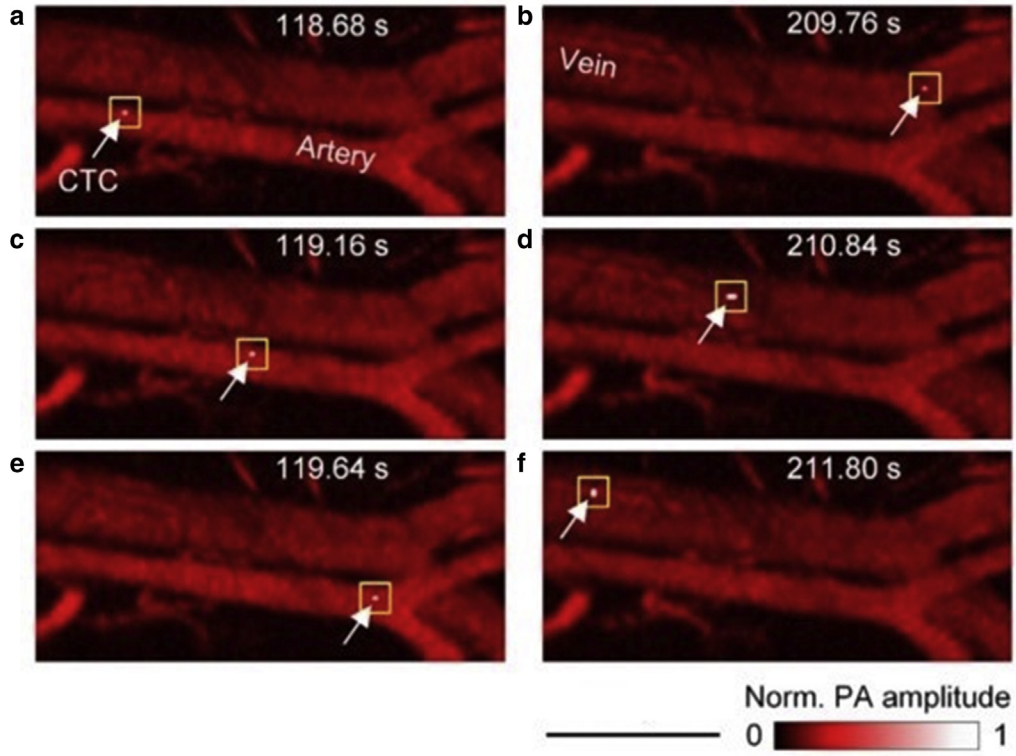

Figure 8. PAT of melanoma CTC in vivo. Three fused OR-PAM images spanning ~3 s show a single melanoma CTC traveling in the artery and then returning in the vein. The yellow boxes indicate the single CTC acquired by OR-PAM at 1,064 nm. Bar = 200 μm. Reprinted with permission from He et al. (2016). CTC, circulating tumor cell; Norm., normal; OR-PAM, optical-resolution photoacoustic microscopy; PA, photoacoustic; PAT, photoacoustic tomography; s, second.

brownish in color, characteristic of burn tissue (Talbert et al., 2007). Edema is another biomarker of thermal damage to the skin because increased blood vessel permeability at the burn site leads to abnormal accumulation of water. Yoshida et al. (2010) have used PAT to successfully characterize edema in burned rat skin, allowing better evaluation of the risks for multiple organ dysfunction syndrome and systemic inflammatory response syndrome. In this study, 1,430 nm excitation light was used, at which water absorbs strongly. Moreover, PAT can be used to trace albumin, the most abundant protein in the blood, to study changes in the permeability of burned skin. For example, Tsunoi et al. (2013) used PAT to image the extravascular leakage of Evans blue dye as the exogenous contrast that binds albumin with a high affinity. In addition to providing diagnostic assistance, PAT can also be used to monitor the healing process of burned or other skin wounds. Später et al. (2017) used PAT to study the lipid-derived microvascular debris density required to reconstruct the host blood vessels. In addition, different tissue conditions such as angiogenesis and healing can be evaluated using PAT in a periodic manner, taking advantage of its noninvasive nonionizing nature (Aizawa et al., 2008). For laser microsurgery, PAT can be used to monitor the vasculature injury and healing process (Hu et al., 2009b). For treating burn tissue infection by antibacterial photodynamic therapy, PAT can be used to map the photosensitizer distribution in the skin to ensure adequate diffusion over the entire infected area (Hirao et al., 2010; Tsunoi et al., 2012).

PAT of single cells in the skin. High-resolution imaging of single cells and cell organelles is crucial in early disease diagnosis. For example, circulating tumor cells (CTCs) are cancerous cells that enter the blood circulation from primary or metastatic lesions and play an important role in tumor recurrence and metastasis (Karakousis et al., 2013). Detection of CTCs has high clinical value for cancer staging. OR-PAM, with submicrometer to micrometer resolution, is well-suited for imaging single-melanoma cell morphology and functions (Strohm et al., 2015). Owing to the rare occurrence of melanoma CTCs in early-stage cancer, blood test–based ex vivo detection of CTCs is incredibly challenging with a small volume of blood sample. Alternatively, on-site PA cytometry can be used to detect the melanoma CTCs without drawing blood (Galanzha et al., 2009). O'Brien et al. (2012) used microfluidic two-phase flow in vitro to separate circulating melanoma tumor cells from the bloodstream on PA detection of melanin. Juratli et al. (2013) discovered that using PA flow cytometry, head and neck melanomas release extra tumor cells into the bloodstream on disturbance by palpation or biopsy. More recently, He et al. (2016) showed single-melanoma CTC detection in vivo, followed by immediate laser ablation of the CTCs (Figure 8).

In addition to pigmented CTCs, PAT has also been used to detect nonpigmented circulating cells (Bhattacharyya et al., 2016; Cai et al., 2016; Galanzha et al., 2015). de la Zerda et al. (2011) have shown PA flowmetry of circulating breast cancer cells using targeted gold nanoparticles. PA flow cytometry has also been applied in the human cuticle for visualization of single red blood cells, which are indicative of overall blood perfusion and vascular health. Hsu et al. (2016) tracked the oxygen saturation and flow speed of each red blood cells as they traveled through the capillary beds. PA and photothermal flow cytometry of the blood and lymph has also been shown for tracking particles besides melanin and

hemoglobin (Galanzha et al., 2007; Tuchin, 2014). Moreover, for skin cell morphology, OR-PAM is capable of performing single-cell histology without staining by imaging DNA and RNA within the cell nuclei and cytochromes within the cytoplasm. For cell functions, PA flowmetry is capable of label-free imaging of oxygen unloading in single red blood cells in vivo (Wang et al., 2013). OR-PAM can image the mitosis of living mesenchymal stem cells, labeled with gold nanoparticles, over 7 days (Zhang et al., 2013). Using the temperature dependence of the PA signal, OR-PAM can measure the temperature of living cells loaded with iron oxide nanoparticles (Gao et al., 2013a, 2013b).

Discussion and outlook

As the largest organ of the human body, the skin is the most accessible organ for PA imaging. PAT is capable of multiscale imaging with consistent optical absorption contrast, providing anatomical, functional, and molecular information in scattering living tissue. This capability has permitted biomedical studies that require high-resolution images at depths beyond the human skin and filled a void between the traditional microscopic and macroscopic imaging methods used in dermatology. The noninvasiveness of PAT has further allowed longitudinal imaging of morphological and functional changes in skin diseases, enabling analysis of the experimental observations and clinical examination in a larger temporal context. In turn, skin imaging is also one of the most promising paths for translation of PA imaging from a benchtop laboratory technology to a true clinical tool of choice. The strong momentum of PAT development is fueled by its increasingly popular applications in skin imaging. In fact, a great effort has been made to develop real-time, modifiable PA imaging systems that can be easily tailored to a given patient's condition in a clinical setting (Kim et al., 2020).

The advancements in PAT technologies signify great potential for clinical or research-based skin imaging. The preclinical and clinical applications reviewed in this paper are highly representative of the current state of PA skin imaging technologies. Many technological challenges still remain, but few are beyond reach. Each PAT implementation has specific strengths toward particular clinical and research applications. As PA imaging becomes more translational, the safety and cost considerations of the system will play a greater role in its continued development. Currently, the most significant barrier to PAT's commercial entry is Food and Drug Administration (FDA) regulation and clinical approval, determined by the quality control and safety measures. To translate PAT to clinical skin imaging, the imaging quality in different patient groups (e.g., skin colors, ages, sex) needs to be consistent, providing clinically robust diagnosis information. Developing a rigorous and well-accepted testing system (e.g., skin phantoms, resolution targets, molecular probes) to evaluate the imaging technologies is also crucial before moving on to human studies. In one such effort, a stable phantom was developed from polyvinyl chloride plastisol to evaluate the precision of different PAT instruments (Bohndiek et al., 2013).

The safety of PAT systems for skin imaging is another area of concern. Endogenous contrasts, such as hemoglobin, melanin, and lipids, are by nature biologically safe (Mehrmohammadi et al., 2013). Successful PA applications should take advantage of endogenous contrasts over exogenous ones to accelerate the regulatory process. However, if exogenous contrasts must be employed, PAT systems have also shown great success in monitoring microneedle delivery of nanoparticles (Moothanchery et al., 2017). The laser system is another important safety concern. Although studies have been performed to elucidate the necessary energy requirements for high-quality skin imaging (Schwarz et al., 2017), the output is ultimately limited by the American National Standards Institute, which specifies a maximum exposure limit of 26.4 mJ/cm^2 on the skin surface at 760 nm (Laser Institute of America, 2007). For dark-skinned patients, the relatively high concentration of melanin poses a challenge for PAT because the skin of these patients is more optically absorbing and thus might be prone to photothermal damage. Potential solutions include the application of transparent coolant to the skin surface while performing PA imaging or clearing the skin surface using a NIR laser. One recent safety advancement in PA skin imaging is the use of more cost-effective and compact excitation sources such as diode lasers (Heres et al., 2017; Zeng et al., 2015) and class I lasers (Bost et al., 2014), which have much lower energy levels than traditional classes III and IV lasers. Translational efforts have even seen the modification of other components of PA systems such as the creation of human skin–adapted probes (Ma et al., 2017). The cost and safety advantages of low-power light sources will likely be extremely advantageous during clinical translation. As the developers of PAT continue focusing on quality control, efficient light delivery, multimodality integration, and safe contrast agents, PAT will further advance toward clinical approval and adoption by physicians and scientists for broad applications on skins. With more commercially available PAT systems tailored for clinical skin imaging, the user base will also experience a fast expansion in the next several years, resulting in a large number of published clinical studies. Of particular importance is the first FDA-approved PAT system by Seno Medical Instruments, Inc (San Antonio, TX), which has paved the way for more commercial PAT systems to receive regulatory clearance.

Meanwhile, it is critically important to identify killer applications in skin imaging that can pilot the technology throughout the translational process. Many skin diseases are essentially blood vessel diseases, and PAT can be used to inform diagnostic and treatment decisions on the basis of the skin vessel conditions. One of the most promising candidates, cutaneous small-vessel vasculitis (CSVV), is a common skin vascular disease. In CSVV, the diseased skin shows red blood cell extravasation, fibrin deposition, and disruption of the vessel wall (Takatu et al., 2017). CSVV can occur at anatomical locations that might be difficult to access, such as the neck, arm, and face. Imaging the cutaneous vasculature functions using PAT, in combination with a skin biopsy, will allow dermatologists to better evaluate the severity of the cutaneous disease and discover any accompanying systemic small vessel involvement. Understanding the dynamics of vascular functions in various skin diseases, such as microvessel density, blood flow, and oxygenation, which cannot be biopsied, will provide knowledge that is crucial for

monitoring disease progression and response to therapy. The knowledge gained from PAT may also be applicable to severe vasculitic or vasculopathic disease models, such as dermatomyositis or scleroderma, in which biopsy of the affected area (in both cases, the tips of the fingers) may not be feasible. We envision that PAT of skin tissues will serve as a valuable surrogate to predict and correlate with vascular disruption in other internal organs such as kidneys and lungs that are difficult to assess.

All in all, with its unique imaging capability, PAT has been advancing quickly toward practical impact in healthcare, both in the technology development and in the clinical translation. We expect that PAT will become a technology of choice for diagnosing skin diseases in the near future.

ORCIDs

Daiwei Li: http://orcid.org/0000-0002-0423-6390
Lucas Humayun: http://orcid.org/0000-0003-4624-2550
Emelina Vienneau: http://orcid.org/0000-0002-8759-0837
Tri Vu: http://orcid.org/0000-0002-1384-8647
Junjie Yao: http://orcid.org/0000-0002-2381-706X

AUTHOR CONTRIBUTIONS

Conceptualization: JY; Writing - Original Draft Preparation: DL, LH, EV, TV, JY; Writing - Review and Editing: DL, LH, JY

ACKNOWLEDGMENTS

This work was partially supported by National Institutes of Health grants (R01 EB028143, R01 NS111039, RF1 NS115581, R01GM134036, R21 EB027304, R21EB027981, R43 CA243822, R43 CA239830, R44 HL138185), Duke Institute of Brain Science Incubator Award, American Heart Association Collaborative Sciences Award (18CSA34080277), and Chan Zuckerberg Initiative Grant 2020-226178 by Silicon Valley Community Foundation. We thank Caroline Connor for editing the manuscript.

CONFLICT OF INTEREST

The authors state no conflict of interest.

REFERENCES

Aguirre J, Schwarz M, Garzorz N, Omar M, Buehler A, Eyerich K, et al. Precision assessment of label-free psoriasis biomarkers with ultra-broadband optoacoustic mesoscopy. Nat Biomed Eng 2017;1:1–8.

Aizawa K, Sato S, Saitoh D, Ashida H, Obara M. Photoacoustic monitoring of burn healing process in rats. J Biomed Opt 2008;13:064020.

Argenziano G, Zalaudek I, Corona R, Sera F, Cicale L, Petrillo G, et al. Vascular structures in skin tumors: a dermoscopy study. Arch Dermatol 2004;140:1485–9.

Arrasmith CL, Dickensheets DL, Mahadevan-Jansen A. MEMS-based hand-held confocal microscope for in-vivo skin imaging. Opt Express 2010;18:3805–19.

Attia ABE, Balasundaram G, Moothanchery M, Dinish US, Bi R, Ntziachristos V, et al. A review of clinical photoacoustic imaging: current and future trends. Photoacoustics 2019;16:100144.

Beard P. Biomedical photoacoustic imaging. Interface Focus 2011;1:602–31.

Bhattacharyya K, Goldschmidt BS, Viator JA. Detection and capture of breast cancer cells with photoacoustic flow cytometry. J Biomed Opt 2016;21:87007.

Bitton R, Zemp R, Yen J, Wang LV, Shung KK. A 3-D high-frequency array based 16 channel photoacoustic microscopy system for in vivo micro-vascular imaging. IEEE Trans Med Imaging 2009;28:1190–7.

Bohndiek SE, Bodapati S, Van De Sompel D, Kothapalli SR, Gambhir SS. Development and application of stable phantoms for the evaluation of photoacoustic imaging instruments. PLoS One 2013;8:e75533.

Bost W, Lemor R, Fournelle M. Optoacoustic imaging of subcutaneous microvasculature with a class one laser. IEEE Trans Med Imaging 2014;33:1900–4.

Braverman IM, Yen A. Ultrastructure of the capillary loops in the dermal papillae of psoriasis. J Invest Dermatol 1977;68:53–60.

Breathnach A, Concannon L, Aalto L, Dorairaj J, Subhash HM, Kelly J, et al. Assessment of cutaneous melanoma and pigmented skin lesions with photoacoustic imaging. In: Kang HW, Wong BJ, Ilgner JF, Nuttal A, Richter CP, Skala MC, et al., editors. Photonic therapeutics and diagnostics XI, proceedings, vol. 9303. Bellingham, WA: SPIE Press; 2015:930303.

Cai C, Carey KA, Nedosekin DA, Menyaev YA, Sarimollaoglu M, Galanzha EI, et al. In vivo photoacoustic flow cytometry for early malaria diagnosis. Cytometry A 2016;89:531–42.

Calzavara-Pinton P, Longo C, Venturini M, Sala R, Pellacani G. Reflectance confocal microscopy for in vivo skin imaging. Photochem Photobiol 2008;84:1421–30.

Chen SL, Ling T, Huang SW, Won Baac H, Guo LJ. Photoacoustic correlation spectroscopy and its application to low-speed flow measurement. Opt Lett 2010;35:1200–2.

Choi W, Park EY, Jeon S, Kim C. Clinical photoacoustic imaging platforms. Biomed Eng Lett 2018;8:139–55.

Chuah SY, Attia AB, Long V, Ho CJ, Malempati P, Fu CY, et al. Structural and functional 3D mapping of skin tumours with non-invasive multispectral optoacoustic tomography. Skin Res Technol 2017;23:221–6.

Cox B, Laufer JG, Arridge SR, Beard PC. Quantitative spectroscopic photoacoustic imaging: a review. J Biomed Opt 2012;17:061202.

Crowe CS, Massenburg BB, Morrison SD, Naghavi M, Pham TN, Gibran NS. Trends of burn injury in the United States: 1990 to 2016. Ann Surg 2019;270:944–53.

Davis LE, Shalin SC, Tackett AJ. Current state of melanoma diagnosis and treatment. Cancer Biol Ther 2019;20:1366–79.

de la Zerda A, Kim JW, Galanzha EI, Gambhir SS, Zharov VP. Advanced contrast nanoagents for photoacoustic molecular imaging, cytometry, blood test and photothermal theranostics. Contrast Media Mol Imaging 2011;6:346–69.

de la Zerda A, Liu Z, Bodapati S, Teed R, Vaithilingam S, Khuri-Yakub BT, et al. Ultrahigh sensitivity carbon nanotube agents for photoacoustic molecular imaging in living mice. Nano Lett 2010;10:2168–72.

Deán-Ben XL, Razansky D. Hand-held optoacoustic probe for three-dimensional imaging of human morphology and function. In: Oraevsky AA, Wang LV, editors. Photons plus ultrasound: imaging and sensing 2014, proceedings, vol. 8943. Bellingham, WA: SPIE; 2014. p. 68–73.

Erpelding TN, Kim C, Pramanik M, Jankovic L, Maslov K, Guo ZJ, et al. Sentinel lymph nodes in the rat: noninvasive photoacoustic and US imaging with a clinical US system. Radiology 2010;256:102–10.

Favazza C, Maslov K, Cornelius L, Wang LV. In vivo functional human imaging using photoacoustic microscopy: response to ischemic and thermal stimuli. In: Oraevsky AA, Wang LV, editors. Photons plus ultrasound: imaging and sensing 2010, proceedings, vol. 7564. Bellingham, WA: SPIE Press; 2010:75640Z.

Favazza CP, Cornelius LA, Wang LV. In vivo functional photoacoustic microscopy of cutaneous microvasculature in human skin. J Biomed Opt 2011;16:026004.

Funasaka Y, Mayumi N, Asayama S, Takayama R, Kosaka M, Kato T, et al. In vivo reflectance confocal microscopy for skin imaging in melasma. J Nippon Med Sch 2013;80:172–3.

Galanzha EI, Nedosekin DA, Sarimollaoglu M, Orza AI, Biris AS, Verkhusha VV, et al. Photoacoustic and photothermal cytometry using photoswitchable proteins and nanoparticles with ultrasharp resonances [published correction appears in J Biophotonics 2015;8:687]. J Biophotonics 2015;8:81–93.

Galanzha EI, Shashkov EV, Kelly T, Kim JW, Yang L, Zharov VP. In vivo magnetic enrichment and multiplex photoacoustic detection of circulating tumour cells. Nat Nanotechnol 2009;4:855–60.

Galanzha EI, Tuchin VV, Brock RW, Zharov VP. In vivo flow cytometry and time-resolved near-IR angiography and lymphography. In: Tuchin VV, editor. Saratov Fall Meeting 2006: Optical technologies in biophysics and medicine VIII, vol. 6535. Bellingham, WA: SPIE—The International Society for Optical Engineering; 2007:65350K.

Gao L, Wang L, Li C, Liu Y, Ke H, Zhang C, et al. Single-cell photoacoustic thermometry. J Biomed Opt 2013a;18:26003.

Gao L, Zhang C, Li C, Wang LV. Intracellular temperature mapping with fluorescence-assisted photoacoustic-thermometry. Appl Phys Lett 2013b;102:193705.

Ghita MA, Caruntu C, Rosca AE, Kaleshi H, Caruntu A, Moraru L, et al. Reflectance confocal microscopy and dermoscopy for in vivo, non-invasive skin imaging of superficial basal cell carcinoma. Oncol Lett 2016;11:3019–24.

Gröhl J, Schellenberg M, Dreher K, Maier-Hein L. Deep learning for biomedical photoacoustic imaging: a review. Photoacoustics 2021;22:100241.

Guo ZJ, Hu S, Wang LV. Calibration-free absolute quantification of optical absorption coefficients using acoustic spectra in 3D photoacoustic microscopy of biological tissue. Opt Lett 2010;35:2067–9.

Haven NJ, Kedarisetti P, Restall BS, Zemp RJ. Reflective objective-based ultraviolet photoacoustic remote sensing virtual histopathology. Opt Lett 2020;45:535–8.

He Y, Wang L, Shi J, Yao J, Li L, Zhang R, et al. In vivo label-free photoacoustic flow cytography and on-the-spot laser killing of single circulating melanoma cells. Sci Rep 2016;6:39616.

Heidenreich R, Röcken M, Ghoreschi K. Angiogenesis drives psoriasis pathogenesis. Int J Exp Pathol 2009;90:232–48.

Heres HM, Arabul MU, Rutten MC, Van de Vosse FN, Lopata RG. Visualization of vasculature using a hand-held photoacoustic probe: phantom and in vivo validation. J Biomed Opt 2017;22:41013.

Hieken TJ, Hernández-Irizarry R, Boll JM, Jones Coleman JE. Accuracy of diagnostic biopsy for cutaneous melanoma: implications for surgical oncologists. Int J Surg Oncol 2013;2013:196493.

Hindelang B, Aguirre J, Berezhnoi A, He H, Eyerich K, Ntziachristos V, et al. Optoacoustic mesoscopy shows potential to increase accuracy of allergy patch testing. Contact Dermatitis 2020;83:206–14.

Hirao A, Sato S, Saitoh D, Shinomiya N, Ashida H, Obara M. In vivo photoacoustic monitoring of photosensitizer distribution in burned skin for antibacterial photodynamic therapy. Photochem Photobiol 2010;86:426–30.

Hsu HC, Wang LD, Wang LV. In vivo photoacoustic microscopy of human cuticle microvasculature with single-cell resolution. J Biomed Opt 2016;21:56004.

Hu S, Maslov K, Tsytsarev V, Wang LV. Functional transcranial brain imaging by optical-resolution photoacoustic microscopy. J Biomed Opt 2009a;14:040503.

Hu S, Maslov KI, Wang LV. Monitoring the healing process of laser-induced microvascular lesions using optical-resolution photoacoustic microscopy. In: Oraevsky AA, Wang LV, editors. Photons plus ultrasound: imaging and sensing 2009, proceedings, vol. 7177. Bellingham, WA: SPIE; 2009b:71772I.

Hu S, Wang LV. Photoacoustic imaging and characterization of the microvasculature. J Biomed Opt 2010;15:011101.

Ida T, Iwazaki H, Kawaguchi Y, Kawauchi S, Ohkura T, Iwaya K, et al. Burn depth assessments by photoacoustic imaging and laser Doppler imaging. Wound Repair Regen 2016;24:349–55.

James WD, Elston DM, Berger TG. Andrews' diseases of the skin: clinical dermatology. Amsterdam, The Netherlands: Elsevier; 2016.

Jennette JC, Falk RJ. Small-vessel vasculitis. N Engl J Med 1997;337:1512–23.

Jeon M, Kim J, Kim C. Multiplane spectroscopic whole-body photoacoustic imaging of small animals in vivo. Med Biol Eng Comput 2016;54:283–94.

Jiao S, Jiang M, Hu J, Fawzi A, Zhou Q, Shung KK, et al. Photoacoustic ophthalmoscopy for in vivo retinal imaging. Opt Express 2010;18:3967–72.

Juratli MA, Galanzha EI, Sarimollaoglu M, Nedosekin DA, Suen JY, Zharov VP. In vivo detection of circulating tumor cells during tumor manipulation. In: Mandelis A, Wong BJF, Ilgner JF, Mahadevan-Jansen A, Jansen ED, Hirschberg H, et al., editors. Photonic therapeutics and diagnostics IX, proceedings, vol. 8565. Bellingham, WA: SPIE; 2013:85652H.

Karakousis G, Yang R, Xu X. Circulating melanoma cells as a predictive biomarker. J Invest Dermatol 2013;133:1460–2.

Kim C, Favazza C, Wang LV. In vivo photoacoustic tomography of chemicals: high-resolution functional and molecular optical imaging at new depths. Chem Rev 2010;110:2756–82.

Kim J, Kim YH, Park B, Seo HM, Bang CH, Park GS, et al. Multispectral ex vivo photoacoustic imaging of cutaneous melanoma for better selection of the excision margin. Br J Dermatol 2018;179:780–2.

Kim J, Park EY, Park B, Choi W, Lee KJ, Kim C. Towards clinical photoacoustic and ultrasound imaging: probe improvement and real-time graphical user interface. Exp Biol Med (Maywood) 2020;245:321–9.

Kim WB, Jerome D, Yeung J. Diagnosis and management of psoriasis. Can Fam Physician 2017;63:278–85.

Laser Institute of America. American National Standards Institute - Z136.1: safe use of lasers. https://www.lia.org/resources/laser-safety-information/laser-safety-standards/ansi-z136-standards/z136-1; 2007 (accessed 1 April 2021).

Lazzarini R, Duarte I, Ferreira AL. Patch tests. An Bras Dermatol 2013;88:879–88.

Leder HA, Campbell JP, Sepah YJ, Gan T, Dunn JP, Hatef E, et al. Ultra-wide-field retinal imaging in the management of non-infectious retinal vasculitis. J Ophthalmic Inflamm Infect 2013;3:30.

Lee C, Choi W, Kim J, Kim C. Three-dimensional clinical handheld photoacoustic/ultrasound scanner. Photoacoustics 2020;18:100173.

Li L, Zhang HF, Zemp RJ, Maslov K, Wang L. Simultaneous imaging of a lacZ-marked tumor and microvasculature morphology in vivo by dual-wavelength photoacoustic microscopy. J Innov Opt Health Sci 2008a;1:207–15.

Li M, Oh JT, Xie X, Ku G, Wang W, Li C, et al. Simultaneous molecular and hypoxia imaging of brain tumors in vivo using spectroscopic photoacoustic tomography. Proc IEEE 2008b;96:481–9.

Li ML, Wang JC, Schwartz JA, Gill-Sharp KL, Stoica G, Wang LV. In-vivo photoacoustic microscopy of nanoshell extravasation from solid tumor vasculature. J Biomed Opt 2009;14:010507.

Li Y, Gonzalez S, Terwey TH, Wolchok J, Li Y, Aranda I, et al. Dual mode reflectance and fluorescence confocal laser scanning microscopy for in vivo imaging melanoma progression in murine skin. J Invest Dermatol 2005;125:798–804.

Liao LD, Li ML, Lai HY, Shih YY, Lo YC, Tsang S, et al. Imaging brain hemodynamic changes during rat forepaw electrical stimulation using functional photoacoustic microscopy. Neuroimage 2010;52:562–70.

Lin L, Zhang P, Xu S, Shi J, Li L, Yao J, et al. Handheld optical-resolution photoacoustic microscopy. J Biomed Opt 2017;22:41002.

Ma H, Cheng Z, Wang Z, Zhang W, Yang S. Switchable optical and acoustic resolution photoacoustic dermoscope dedicated into in vivo biopsy-like of human skin. Appl Phys Lett 2020;116:073703.

Ma H, Yang S, Cheng Z, Xing D. Photoacoustic confocal dermoscope with a waterless coupling and impedance matching opto-sono probe. Opt Lett 2017;42:2342–5.

Maconi G, Imbesi V, Bianchi Porro G. Doppler ultrasound measurement of intestinal blood flow in inflammatory bowel disease. Scand J Gastroenterol 1996;31:590–3.

Manohar S, Razansky D. Photoacoustics: a historical review. Adv Opt Photonics 2016;8:586–617.

Martin SF. Contact dermatitis: from pathomechanisms to immunotoxicology. Exp Dermatol 2012;21:382–9.

Maslov K, Stoica G, Wang LV. In vivo dark-field reflection-mode photoacoustic microscopy. Opt Lett 2005;30:625–7.

Maslov K, Zhang HF, Hu S, Wang LV. Optical-resolution photoacoustic microscopy for in vivo imaging of single capillaries. Opt Lett 2008;33:929–31.

Matteson EL. Small-vessel vasculitis. N Engl J Med 1998;338:994–5.

Mehrmohammadi M, Yoon SJ, Yeager D, Emelianov SY. Photoacoustic imaging for cancer detection and staging. Curr Mol Imaging 2013;2:89–105.

Miller AJ, Mihm MC Jr. Melanoma. N Engl J Med 2006;355:51–65.

Moothanchery M, Seeni RZ, Xu C, Pramanik M. In vivo studies of transdermal nanoparticle delivery with microneedles using photoacoustic microscopy. Biomed Opt Express 2017;8:5483–92.

Morris DO, Beale KM. Cutaneous vasculitis and vasculopathy. Vet Clin North Am Small Anim Pract 1999;29:1325–35.

O'Brien CM, Rood KD, Bhattacharyya K, DeSouza T, Sengupta S, Gupta SK, et al. Capture of circulating tumor cells using photoacoustic flowmetry and two phase flow. J Biomed Opt 2012;17:061221.

Oh JT, Li ML, Zhang HF, Maslov K, Stoica G, Wang LV. Three-dimensional imaging of skin melanoma in vivo by dual-wavelength photoacoustic microscopy. J Biomed Opt 2006;11:34032.

Oladipupo S, Hu S, Kovalski J, Yao J, Santeford A, Sohn RE, et al. VEGF is essential for hypoxia-inducible factor-mediated neovascularization but dispensable for endothelial sprouting. Proc Natl Acad Sci USA 2011a;108:13264–9.

Oladipupo SS, Hu S, Santeford AC, Yao J, Kovalski JR, Shohet RV, et al. Conditional HIF-1 induction produces multistage neovascularization with stage-specific sensitivity to VEGFR inhibitors and myeloid cell independence. Blood 2011b;117:4142–53.

Olafsson R, Bauer DR, Montilla LG, Witte RS. Real-time, contrast enhanced photoacoustic imaging of cancer in a mouse window chamber. Opt Express 2010;18:18625–32.

Omar M, Schwarz M, Soliman D, Symvoulidis P, Ntziachristos V. Pushing the optical imaging limits of cancer with multi-frequency-band raster-scan optoacoustic mesoscopy (RSOM). Neoplasia 2015;17:208–14.

Ossadnik K, Philipp S, Bost W, Fournelle M, Richter H, Lademann J. Application of photoacoustic methods and confocal microscopy for monitoring of therapeutic response in plaque psoriasis. Skin Pharmacol Physiol 2018;31:308–15.

Park B, Bang CH, Lee C, Han JH, Choi W, Kim J, et al. 3D wide-field multispectral photoacoustic imaging of human melanomas in vivo: a pilot study. J Eur Acad Dermatol Venereol 2021;35:669–76.

Patrikeev I, Brecht HP, Petrov YY, Petrova IY, Prough DS, Esenaliev RO. Wavelet differentiation of optoacoustic signals for monitoring of total hemoglobin concentration and oxygen saturation level in small blood vessels. In: Oraevsky AA, Wang LV, editors. Photons plus ultrasound: imaging and sensing 2007: the Eighth Conference on Biomedical Thermoacoustics, Optoacoustics, and Acousto-Optics, proceedings, vol. 6437. Bellingham, WA: SPIE; 2007:643717.

Pleitez MA, Khan AA, Soldà A, Chmyrov A, Reber J, Gasparin F, et al. Label-free metabolic imaging by mid-infrared optoacoustic microscopy in living cells. Nat Biotechnol 2020;38:293–6.

Proksch E, Brandner JM, Jensen JM. The skin: an indispensable barrier. Exp Dermatol 2008;17:1063–72.

Rahlves M, Varkentin A, Stritzel J, Blumenrother E, Mazurenka M, Wollweber M, et al. Towards multimodal detection of melanoma thickness based on Optical Coherence Tomography and Optoacoustics. In: Azar FS, Intes X, editors. Multimodal biomedical imaging XI: 13 February 2016, San Francisco, California, United States, proceedings, vol. 9701. Bellingham, WA: SPIE; 2016:97010F.

Raza K, Thambyrajah J, Townend JN, Exley AR, Hortas C, Filer A, et al. Suppression of inflammation in primary systemic vasculitis restores vascular endothelial function: lessons for atherosclerotic disease? Circulation 2000;102:1470–2.

Rendon A, Schäkel K. Psoriasis pathogenesis and treatment. Int J Mol Sci 2019;20:1475.

Rowland KJ, Yao J, Wang L, Erwin CR, Maslov KI, Wang LV, et al. Immediate alterations in intestinal oxygen saturation and blood flow after massive small bowel resection as measured by photoacoustic microscopy. J Pediatr Surg 2012;47:1143–9.

Ryan TJ. Microcirculation in psoriasis: blood vessels, lymphatics and tissue fluid. Pharmacol Ther 1980;10:27–64.

Sato S, Shimada T, Arai T, Kikuchi M, Obara M, Ashida H. Measurement of photoacoustic signals from skin: potential application to burn depth estimation. In: Boccara AC, Oraevsky AA, editors. Hybrid and novel imaging and new optical instrumentation for biomedical applications, proceedings, vol. 4434. Bellingham, WA: SPIE; 2001. p. 8–12.

Sato S, Yamazaki M, Saitoh D, Tsuda H, Okada Y, Obara M, et al. Photoacoustic diagnosis of burns in rats. J Trauma 2005;59:1450–5.

Schmidt WA. Imaging in vasculitis. Best Pract Res Clin Rheumatol 2013;27:107–18.

Schwarz M, Aguirre J, Buehler A, Omar M, Ntziachristos V. Visualization of the microcirculatory network in skin by high frequency optoacoustic mesoscopy. In: Ntziachristos V, Zemp R, editors. Opto-acoustic methods and applications in biophotonics II, proceedings, vol. 9539. Bellingham, WA: SPIE; 2015:95390J.

Schwarz M, Soliman D, Omar M, Buehler A, Ovsepian SV, Aguirre J, et al. Optoacoustic dermoscopy of the human skin: tuning excitation energy for optimal detection bandwidth with fast and deep imaging in vivo. IEEE Trans Med Imaging 2017;36:1287–96.

Seth D, Cheldize K, Brown D, Freeman EF. Global burden of skin disease: inequities and innovations. Curr Dermatol Rep 2017;6:204–10.

Shi J, Wong TTW, He Y, Li L, Zhang R, Yung CS, et al. High-resolution, high-contrast mid-infrared imaging of fresh biological samples with ultraviolet-localized photoacoustic microscopy. Nat Photonics 2019;13:609–15.

Silverman RH, Kong F, Chen YC, Lloyd HO, Kim HH, Cannata JM, et al. High-resolution photoacoustic imaging of ocular tissues. Ultrasound Med Biol 2010;36:733–42.

Song W, Wei Q, Liu T, Kuai D, Burke JM, Jiao S, et al. Integrating photoacoustic ophthalmoscopy with scanning laser ophthalmoscopy, optical coherence tomography, and fluorescein angiography for a multimodal retinal imaging platform. J Biomed Opt 2012;17:061206.

Später T, Körbel C, Frueh FS, Nickels RM, Menger MD, Laschke MW. Seeding density is a crucial determinant for the in vivo vascularisation capacity of adipose tissue-derived microvascular fragments. Eur Cell Mater 2017;34:55–69.

Staley J, Grogan P, Samadi AK, Cui H, Cohen MS, Yang X. Growth of melanoma brain tumors monitored by photoacoustic microscopy. J Biomed Opt 2010;15:040510.

Steingräber AK, Schelhaas S, Faust A, Jacobs AH, Schäfers M, Goerge T. Molecular imaging reveals time course of matrix metalloproteinase activity in acute cutaneous vasculitis in vivo. Exp Dermatol 2013;22:730–5.

Strohm EM, Moore MJ, Kolios MC. Single cell photoacoustic microscopy: a review. IEEE J Sel Top Quantum Electron 2015;22:137–51.

Subach FV, Zhang LJ, Gadella TW, Gurskaya NG, Lukyanov KA, Verkhusha VV. Red fluorescent protein with reversibly photoswitchable absorbance for photochromic FRET. Chem Biol 2010;17:745–55.

Takatu CM, Heringer APR, Aoki V, Valente NYS, de Faria Sanchez PC, de Carvalho JF, et al. Clinicopathologic correlation of 282 leukocytoclastic vasculitis cases in a tertiary hospital: a focus on direct immunofluorescence findings at the blood vessel wall. Immunol Res 2017;65:395–401.

Talbert RJ, Holan SH, Viator JA. Photoacoustic discrimination of viable and thermally coagulated blood using a two-wavelength method for burn injury monitoring. Phys Med Biol 2007;52:1815–29.

Taruttis A, Herzog E, Razansky D, Ntziachristos V. Real-time imaging of cardiovascular dynamics and circulating gold nanorods with multispectral optoacoustic tomography. Opt Express 2010;18:19592–602.

Thyssen JP, Linneberg A, Menné T, Johansen JD. The epidemiology of contact allergy in the general population–prevalence and main findings. Contact Dermatitis 2007;57:287–99.

Tsunoi Y, Sato S, Ashida H, Terakawa M. Photoacoustic imaging of intravenously injected photosensitizer in rat burn models for efficient antibacterial photodynamic therapy. In: Kessel DH, Hasan T, editors. Optical methods for tumor treatment and detection: mechanisms and techniques in photodynamic therapy XXI, proceedings, vol. 8210. Bellingham, WA: SPIE; 2012:82100D.

Tsunoi Y, Sato S, Kawauchi S, Ashida H, Saitoh D, Terakawa M. In vivo photoacoustic molecular imaging of the distribution of serum albumin in rat burned skin. Burns 2013;39:1403–8.

Tsytsarev V, Hu S, Yao J, Maslov K, Barbour DL, Wang LV. Photoacoustic microscopy of microvascular responses to cortical electrical stimulation. J Biomed Opt 2011;16:076002.

Tuchin VV. In vivo optical flow cytometry and cell imaging. Rivista del Nuovo Cimento 2014;37:375–416.

Upputuri PK, Pramanik M. Recent advances in photoacoustic contrast agents for in vivo imaging. Wiley Interdiscip Rev Nanomed Nanobiotechnol 2020;12:e1618.

Viator JA, Aguilar G, Jacques SL, Nelson JS. Optimization of cryogen spray cooling for port wine stain laser therapy using photoacoustic measurement of epidermal melanin. Int Mech Eng Congress Expo 2003;37106:13–4.

Viator JA, Au G, Choi B, Nelson JS. Design limitations of a photoacoustic probe for port wine stain depth determination. In: Oraevsky AA, editor. Biomedical Optoacoustics III, vol. 4618. Bellingham, WA: SPIE; 2002a. p. 7–15.

Viator JA, Au G, Paltauf G, Jacques SL, Prahl SA, Ren HW, et al. Clinical testing of a photoacoustic probe for port wine stain depth determination. Lasers Surg Med 2002b;30:141–8.

Viator JA, Kolkman RGM, Steenbergen W. Photoacoustic depth determination and imaging of port wine stain birthmarks. In: Wang LV, editor.

Photoacoustic Imaging and Spectroscopy. Boca Raton, FL: CRC Press; 2009. p. 463–72.

Wang B, Su JL, Karpiouk AB, Sokolov KV, Smalling RW, Emelianov SY. Intravascular photoacoustic imaging. IEEE J Quantum Electron 2010;16: 588–99.

Wang LD, Maslov K, Wang LV. Single-cell label-free photoacoustic flowoxigraphy in vivo. Proc Natl Acad Sci USA 2013;110:5759–64.

Wang LV, Wu HI. Biomedical optics: principles and imaging. Hoboken, NJ: John Wiley & Sons; 2007.

Wang LV, Yao J. A practical guide to photoacoustic tomography in the life sciences. Nat Methods 2016;13:627–38.

Wang XD, Ku G, Wegiel MA, Bornhop DJ, Stoica G, Wang LV. Noninvasive photoacoustic angiography of animal brains in vivo with near-infrared light and an optical contrast agent. Opt Lett 2004;29:730–2.

Wang Y, Xu D, Yang S, Xing D. Toward in vivo biopsy of melanoma based on photoacoustic and ultrasound dual imaging with an integrated detector. Biomed Opt Express 2016;7:279–86.

Wang Z, Yang F, Ma H, Cheng Z, Yang S. Photoacoustic and ultrasound (PAUS) dermoscope with high sensitivity and penetration depth by using a bimorph transducer. J Biophotonics 2020;13:e202000145.

Wong TTW, Zhang R, Hai P, Zhang C, Pleitez MA, Aft RL, et al. Fast label-free multilayered histology-like imaging of human breast cancer by photoacoustic microscopy. Sci Adv 2017a;3:e1602168.

Wong TT, Zhang R, Zhang C, Hsu HC, Maslov KI, Wang L, et al. Label-free automated three-dimensional imaging of whole organs by microtomy-assisted photoacoustic microscopy. Nat Commun 2017b;8:1386.

Xie Z, Jiao S, Zhang HF, Puliafito CA. Laser-scanning optical-resolution photoacoustic microscopy. Opt Lett 2009;34:1771–3.

Xu D, Yang S, Wang Y, Gu Y, Xing D. Noninvasive and high-resolving photoacoustic dermoscopy of human skin. Biomed Opt Express 2016;7: 2095–102.

Xu M, Wang LV. Universal back-projection algorithm for photoacoustic computed tomography [published correction appears in Phys Rev E Stat Nonlin Soft Matter Phys 2007;75:059903]. Phys Rev E Stat Nonlin Soft Matter Phys 2005;71:016706.

Xu Y, Wang LV. Time reversal and its application to tomography with diffracting sources. Phys Rev Lett 2004;92:033902.

Yamazaki M, Sato S, Ashida H, Saito D, Okada Y, Obara M. Measurement of burn depths in rats using multiwavelength photoacoustic depth profiling. J Biomed Opt 2005;10:064011.

Yamazaki M, Sato S, Saito D, Fujita M, Okada Y, Kikuchi M, et al. Photoacoustic signal measurement for burned skins in the spectral range of 500–650nm: experiment with rat burn models. In: Oraevsky AA, editor. Biomedical optoacoustics III, proceedings, vol. 4618. Bellingham, WA: SPIE; 2002. p. 16–21.

Yamazaki M, Sato S, Saito D, Okada Y, Kurita A, Kikuchi M, et al. Photoacoustic diagnosis of burns in rats: two-dimensional photoacoustic imaging of burned tissue. In: Oraevsky AA, editor. Biomedical optoacoustics IV, proceedings, vol. 4960. Bellingham, WA: SPIE; 2003. p. 7–13.

Yang C, Lan H, Gao F, Gao F. Review of deep learning for photoacoustic imaging. Photoacoustics 2021;21:100215.

Yang JM, Chen R, Favazza C, Yao J, Zhou Q, Shung KK, et al. A 2.5-mm outer diameter photoacoustic endoscopic mini-probe based on a highly sensitive PMN-PT ultrasonic transducer. In: Oraevsky AA, Wang LV, editors. Photons plus ultrasound: imaging and sensing 2012, proceedings, vol. 8223. Wellingham, WA: SPIE; 2012a. 82233M–6M.

Yang JM, Favazza C, Chen R, Yao J, Cai X, Maslov K, et al. Toward dual-wavelength functional photoacoustic endoscopy: laser and peripheral optical systems development. In: Oraevsky AA, Wang LV, editors. Photons plus ultrasound: imaging and sensing 2012, proceedings, vol. 8223. Wellingham, WA: SPIE; 2012b. p. 822316–7.

Yang JM, Favazza C, Chen R, Yao J, Cai X, Maslov K, et al. Simultaneous functional photoacoustic and ultrasonic endoscopy of internal organs in vivo. Nat Med 2012c;18:1297–302.

Yao DK, Maslov K, Shung KK, Zhou Q, Wang LV. In vivo label-free photoacoustic microscopy of cell nuclei by excitation of DNA and RNA. Opt Lett 2010a;35:4139–41.

Yao J, Maslov KI, Puckett ER, Rowland KJ, Warner BW, Wang LV. Double-illumination photoacoustic microscopy. Opt Lett 2012a;37:659–61.

Yao J, Maslov KI, Zhang Y, Xia Y, Wang LV. Label-free oxygen-metabolic photoacoustic microscopy in vivo. J Biomed Opt 2011;16:076003.

Yao J, Rowland KJ, Wang L, Maslov KI, Warner BW, Wang LV. Double-illumination photoacoustic microscopy of intestinal hemodynamics following massive small bowel resection. In: Oraevsky AA, Wang LV, editors. Photons plus ultrasound: imaging and sensing 2012, proceedings, vol. 8223. Bellingham, WA: SPIE; 2012b. 82233V–7V.

Yao J, Wang LV. Photoacoustic microscopy. Laser Photonics Rev 2013;7: 758–78.

Yao J, Wang LV. Sensitivity of photoacoustic microscopy. Photoacoustics 2014;2:87–101.

Yao J, Xia J, Wang LV. Multiscale functional and molecular photoacoustic tomography. Ultrason Imaging 2016;38:44–62.

Yao J, Maslov KI, Shi Y, Taber LA, Wang LV. In vivo photoacoustic imaging of transverse blood flow by using Doppler broadening of bandwidth. Opt Lett 2010b;35:1419–21.

Yew YW, Unnimadhava Kurup Soudamini Amma D, Kuan AHY, Li X, Dev K, Ebrahim Attia AB, et al. Raster-scanning optoacoustic mesoscopy imaging as an objective disease severity tool in atopic dermatitis patients. J Am Acad Dermatol 2021;84:1121–3.

Yoshida K, Sato S, Hatanaka K, Saitoh D, Ashida H, Sakamoto T, et al. Photoacoustic diagnosis of edema in rat burned skin. In: Oraevsky AA, Wang LV, editors. Photons plus ultrasound: imaging and sensing 2010, proceedings, vol. 7564. Wellingham, WA: Proceedings of SPIE; 2010:75641C.

Zemp RJ, Song L, Bitton R, Shung KK, Wang LV. Realtime photoacoustic microscopy of murine cardiovascular dynamics. Opt Express 2008;16: 18551–6.

Zeng L, Piao Z, Huang S, Jia W, Chen Z. Label-free optical-resolution photoacoustic microscopy of superficial microvasculature using a compact visible laser diode excitation. Opt Express 2015;23:31026–33.

Zhang C, Maslov K, Wang LV. Subwavelength-resolution label-free photoacoustic microscopy of optical absorption in vivo. Opt Lett 2010;35: 3195–7.

Zhang EZ, Laufer JG, Pedley RB, Beard PC. In vivo high-resolution 3D photoacoustic imaging of superficial vascular anatomy. Phys Med Biol 2009;54:1035–46.

Zhang HF, Maslov K, Oh JT, Stoica G, Wang LV. Functional photoacoustic microscopy in vivo. In: Oraevsky AA, Wang LV, editors. Photons plus ultrasound: imaging and sensing 2006: the Seventh Conference on Biomedical Thermoacoustics, Optoacoustics, and Acousto-Optics, proceedings, vol. 6086. Wellingham, WA: SPIE; 2006a:60861G.

Zhang HF, Maslov K, Sivaramakrishnan M, Stoica G, Wang LHV. Imaging of hemoglobin oxygen saturation variations in single vessels in vivo using photoacoustic microscopy. Appl Phys Lett 2007a;90:053901.

Zhang HF, Maslov K, Stoica G, Wang LV. Functional photoacoustic microscopy for high-resolution and noninvasive in vivo imaging. Nat Biotechnol 2006b;24:848–51.

Zhang HF, Maslov K, Stoica G, Wang LV. Imaging acute thermal burns by photoacoustic microscopy. J Biomed Opt 2006c;11:054033.

Zhang HF, Maslov K, Stoica G, Wang LV. High-resolution burn imaging in pig skin by photoacoustic microscopy. In: Oraevsky AA, Wang LV, editors. Photons plus ultrasound: imaging and sensing 2007: the Eight Conference on Biomedical Thermoacousitcs, Optoacoustics, and Acousto-Optics, proceedings, vol. 6437. Wellingham, WA: SPIE; 2007b.

Zhang YS, Wang Y, Wang L, Cai X, Zhang C, Wang LV, et al. Labeling human mesenchymal stem cells with gold nanocages for in vitro and in vivo tracking by two-photon microscopy and photoacoustic microscopy. Theranostics 2013;3:532–43.

Zhou WT, Chen Z, Yang S, Xing D. Optical biopsy approach to basal cell carcinoma and melanoma based on all-optically integrated photoacoustic and optical coherence tomography. Opt Lett 2017;42:2145–8.

Zhou Y, Li G, Zhu L, Li C, Cornelius LA, Wang LV. Handheld photoacoustic probe to detect both melanoma depth and volume at high speed in vivo. J Biophotonics 2015;8:961–7.